Materials Science and Engineering C 61 (2016) 659–664

Contents lists available at ScienceDirect

Materials Science and Engineering C

journal homepage: www.elsevier.com/locate/msec

Enhanced conjugation stability and blood circulation time of macromolecular gadolinium-DTPA contrast agent

Ratchapol Jenjob [a], Na Kun [b], Jung Yeon Ghee [c], Zheyu Shen [d], Xiaoxia Wu [d], Steve K. Cho [f,*], Don Haeng Lee [c,e], Su-Geun Yang [a,**]

[a] Department of New Drug Development, School of Medicine, Inha University, 2F A-dong, Jeongseok Bldg., Sinheung-dong 3-ga, Jung-gu, Incheon 400-712, Republic of Korea
[b] Department of Biotechnology, The Catholic University of Korea, 43 Jibong-ro, Wonmi-gu, Bucheon-si, Gyeonggi-do 420-743, Republic of Korea
[c] Utah-Inha DDS and Advanced Therapeutics, B-403 Meet-You-All Tower, SongdoTechnopark, 7–50, Songdo-dong, Yeonsu-gu, Incheon 406-840, Republic of Korea
[d] Division of Functional Materials and Nano-Devices, Ningbo Institute of Materials Technology & Engineering (NIMTE), Chinese Academy of Sciences, 519 Zhuangshi Street, Zhenhai District, Ningbo, Zhejiang 315201, China
[e] Department of Internal Medicine, School of Medicine, Inha University Hospital, Incheon 420-751, Republic of Korea
[f] Division of Liberal Arts and Science, GIST College, Gwangju Institute of Science and Technology, Gwangju 500-712, Republic of Korea

ARTICLE INFO

Article history:
Received 15 August 2015
Received in revised form 10 December 2015
Accepted 3 January 2016
Available online 07 January 2016

Keywords:
Gadolinium-DTPA
Nephrogenic fibrosis
Extended blood circulation
Transmetalation
Chelation stability

ABSTRACT

In this study, we prepared macromolecular MR T1 contrast agent: pullulan-conjugated Gd diethylene triamine pentaacetate (Gd-DTPA-Pullulan) and estimated residual free Gd^{3+}, chelation stability in competition with metal ions, plasma and tissue pharmacokinetics, and abdominal MR contrast on rats. Residual free Gd^{3+} in Gd-DTPA-Pullulan was measured using colorimetric spectroscopy. The transmetalation of Gd^{3+} incubated with Ca^{2+} was performed by using a dialysis membrane (MWCO 100–500 Da) and investigated by ICP-OES. The plasma concentration profiles of Gd-DTPA-Pullulan were estimated after intravenous injection at a dose 0.1 mmol/kg of Gd. The coronal-plane abdominal images of normal rats were observed by MR imaging. The content of free Gd^{3+}, the toxic residual form, was less than 0.01%. Chelation stability of Gd-DTPA-Pullulan was estimated, and only 0.2% and 0.00045% of Gd^{3+} were released from Gd-DTPA-Pullulan after 2 h incubation with Ca^{2+} and Fe^{2+}, respectively. Gd-DTPA-Pullulan displayed the extended plasma half-life ($t_{1/2,\alpha} = 0.43$ h, $t_{1/2,\beta} = 2.32$ h), much longer than 0.11 h and 0.79 h of Gd-EOB-DTPA. Abdominal MR imaging showed Gd-DTPA-Pullulan maintained initial MR contrast for 30 min. The extended plasma half-life of Gd-DTPA-Pullulan probably allows the prolonged MR acquisition time in clinic with enhanced MR contrast.

1. Introduction

Magnetic resonance imaging (MRI) is the most powerful technique for clinical diagnosis [1]. Contrast agents are preferentially prescribed to enhance the quality of MR images. Approximately 25–30% of MR imaging is performed with contrast agents to obtain more descriptive images, and most of them are gadolinium-chelated contrast agents. As of 2007, more than 200 million patients have received Gd-based MR agents worldwide [2]. Recently many new functional MR contrast agents have been reported and are entering preclinical and clinical trials. These experimental contrast agents exhibit exceptional tissue-specific contrast for tumors, angiogenesis, arteriosclerosis, etc. But the safety of MR contrast agents, especially for Gd-based contrast agents, has been neglected during the developmental stages.

The US Food and Drug Administration (FDA) first reported the association of nephrogenic systemic fibrosis (NSF) with prior administration of Gd-based MR contrast agents in 2006 [3,4]. More than 215 cases of NSF were reported in 2007 [5]. Most cases were related to severe renal deficiency (stage 4), with a glomerular filtration rate (GFR) of less than 30 ml/min. The administration of Gd-based MR contrast agents, especially to a renal-impaired patient, is now strictly controlled [6,7].

Gadolinium (Gd)-based MR contrast agents are relatively safe in chelated form, but chelated Gd can be trans-metalated in competition with other metal ions (i.e., Ca^{2+}, Zn^{2+}, Cu^{2+}). The trans-metalated Gd has a longer biological half-life than the chelated form, accumulates in tissues, and leads to systemic fibrosis [8–10]. Chelating agents should therefore be precisely designed to sustain strong chelation power against Gd.

The plasma distribution half-life ($T_{1/2,\ alpha}$) of most Gd-based MR contrast agents is around 30 min [11]. A shorter half-life is a beneficial characteristic in terms of safety. However, too-short half-life of Gd-

* Correspondence to: S.K. Cho, Division of Liberal Arts and Science, GIST College, Gwangju Institute of Science and Technology, Cheomdan Gwagiro 123, Buk-gu, Gwangju 500-712, Republic of Korea.
** Correspondence to: S.-G. Yang, Department of New Drug Development, School of Medicine, Inha University, 8F A-dong, Jeongseok Bldg., Sinheung-dong 3-ga, Jung-gu, Incheon 400-712, Republic of Korea.
E-mail addresses: scho@gist.ac.kr (S.K. Cho), Sugeun.Yang@Inha.ac.kr (S.-G. Yang).

http://dx.doi.org/10.1016/j.msec.2016.01.008
0928-4931/

based MR contrast agents does not allow a sufficient MR acquisition time for distinctive diagnostic imaging [12–14]. Macromolecular Gd chelates have a longer blood circulation time and thus act as effective contrast agents in tumor MR imaging [15]. In addition, macromolecular Gd chelates accumulate in the tumor and allow accurate MR imaging [14].

We recently designed a new macromolecular MR contrast agent, Gd-DTPA-conjugated pullulan (Gd-DTPA-Pullulan) [16]. In this study, we estimated chelation stability of Gd-DTPA-Pullulan. The percentage of residual free Gd^{3+} was estimated by colorimetric spectroscopy, and the chelation stability (degree of transmetalation) was determined after co-incubation with Ca^{2+} and Fe^{2+} ions. We also performed a pharmacokinetic study of Gd-DTPA-Pullulan compared with Gd-EOB-DTPA (gadoxetic acid disodium, Primovist®; Bayer Co.). Gd-EOB-DTPA is a commercial hepatocyte-specific MRI contrast agent which preferentially used for detecting focal hepatic lesions and blood pool agent. Plasma-concentration profiles and tissue distribution of Gd-DTPA-Pullulan were estimated. Then abdominal MR imaging was performed in normal rats based on the observed pharmacokinetic characteristics.

2. Materials and methods

2.1. Materials

Pullulan (MW 100,000) was acquired from Tokyo Chemical Industry Co., Ltd. (Tokyo, Japan). Diethylene triaminepentaaceticdianhydride (DTPA), xylenol orange, and $GdCl_3 \cdot 6H_2O$ were purchased from Sigma-Aldrich (St. Louis, MO, USA). All chemicals were reagent grade and used as supplied.

2.2. Synthesis of Gd-DTPA-Pullulan

Gd-DTPA-Pullulan (Fig. 1) was synthesized as described: 150 mg of pullulan (m.w.; 100 k) and 300 mg of DTPA dianhydride were dissolved in 80 mL of dry DMSO; then, the solution was stirred under magnetic stirring for 24 h at room temperature [16]. After the reaction was completed, 20 mL of distilled water was added to stop the reaction. The final solution was dialyzed against distilled water with a 12,000–14,000 MWCO membrane for 3 days and then lyophilized for 3–4 days in a freeze-dry system (FreeZone 4.5; Labconco Co., Kansas City, MO, USA). 100 mg of DTPA-pullulan and 166 mg of $GdCl_3 \cdot 6H_2O$ were then dissolved in 25 mL of distilled water under moderate stirring, and the solution was adjusted to pH 7.0–7.5. The solution was stirred in an oil bath at 50 °C for 4 h. The acquired Gd-DTPA-Pullulan was introduced again into dialysis membrane (MWCO 12,000–14,000) with additional 4 mg of DTPA to remove free Gd^{3+} and then lyophilized. The amount of Gd chelated in Gd-DTPA-Pullulan was evaluated on an inductively coupled plasma-optical emission spectrometer (ICP-OES, Optima 7300 DV; Perkin Elmer, Waltham, MA). Gd-DTPA-Pullulan was diluted with 2% HNO_3 for analysis. The total Gd content of Gd-DTPA-Pullulan and Gd-EOB-DTPA was 24.35 ± 1.12% and 20.75 ± 0.06%, respectively.

2.3. Estimation of residual free Gd^{3+} in Gd-DTPA-Pullulan

Incomplete chelation of Gd^{3+} may result in residual free Gd^{3+} in the system, and free Gd^{3+} produces false-positive strong MR contrast and cytotoxicity [17]. We estimated the content of residual free Gd^{3+} using colorimetric spectroscopy with modification [18]. Briefly, 5 mg samples were dissolved in xylenol orange solution. Xylenol orange solution was made in fresh by dissolving xylenol orange (3 mg) into acetate buffer (250 ml, pH 5.8). Spectra from 300 to 700 nm were collected on an ultraviolet (UV)–visible absorption spectrophotometer (U-2900; Hitachi, Japan) with a slit width of 1.0 nm. The standard spectrum for $GdCl_3 \cdot 6H_2O$ was prepared, and the calibration curve of free Gd^{3+} in the range of 1 ~ 45 μM was acquired based on the ratio of absorbance at 573 and 433 nm (See supplemental Fig. S1).

2.4. Chelation stability of Gd-DTPA-Pullulan after co-incubation with Ca^{2+} and Fe^{2+}

Chelation stability of Gd-DTPA-Pullulan was determined after co-incubation with Fe^{2+} or Ca^{2+} ions, respectively. Five mg of Gd-DTPA-Pullulan were dissolved in distilled water and transferred to a dialysis membrane (MWCO 100–500 Da) containing 1 mM $CaCl_2$ or 3 mM $FeCl_2$, separately, at 37 °C. One milliliter of outside solution was periodically collected and analyzed in an ICP-OES. The experiment was repeated at least three times. The percentage of transmetalation (released Gd^{3+}) was calculated based on the total amount of Gd and plotted against time.

2.5. Intravenous pharmacokinetics of Gd-DTPA-Pullulan

Gd-DTPA-Pullulan and Gd-EOB-DTPA were intravenously injected into BALB/c mice (n = 6) at a dose of 0.1 mmol/kg of Gd. Gd-DTPA-Pullulan was dissolved in injectable normal saline and injected via the tail vein. Approximately 80 μL of blood from the retro-orbital sinus were withdrawn using a heparinized capillary tube at 1, 15, 30, and 60 min and at 3, 5, 8, 24 h after injection. After centrifugation of the

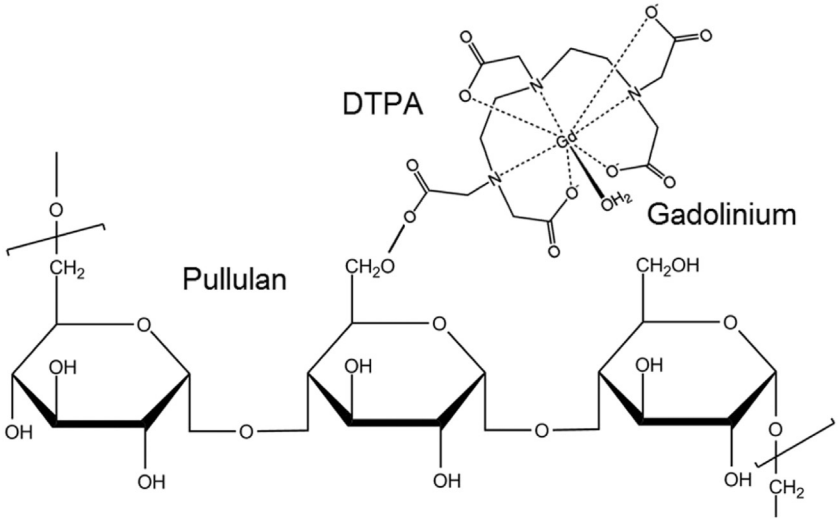

Fig. 1. Chemical structure of pullulan-conjugated gadolinium diethylene triamine pentaacetate (Gd-DTPA-Pullulan).

blood samples, 20 μL of plasma were diluted with 3% ultra-pure nitric acid and analyzed in an ICP-OES.

Plasma concentration-time profiles of Gd-DTPA-Pullulan and Gd-EOB-DTPA were analyzed by the model-dependent method using WinNonlin software (standard v3.1; Pharsight Corp., Cary, NC, USA).

Tissue concentration was also estimated as follows. Mice were sacrificed 3 and 24 h after injection, and immediately perfused with normal saline by heart puncture. Heart, lung, liver, kidney, muscle, and spleen were excised, rinsed in normal saline, and blotted dry on tissue paper. Each tissue sample was weighed, placed in a test tube with distilled water, and homogenized in a tissue homogenizer (Ultra-Turrax T-25; IKA, Germany). Tissue homogenates were diluted with a volume of 60% nitric acid, incubated for 2 days at 60 °C, and centrifuged at 13,000 rpm for 30 min. The supernatant was diluted with 3% ultra-pure nitric acid and subjected to ICP-OES. The Gd concentration in each organ was calculated based on calibration curves that were obtained using organs from non-injected mice and standard stock solution ($GdCl_3 \cdot 6H_2O$).

Animal care and experiments were conducted in accordance with the experimental protocol approved by the ethics committee of the School of Medicine, Inha University, and the Ethical Guidelines for Animal Studies.

2.6. Abdominal MR imaging

Abdominal MR imaging of rats was performed on a 1.5-T MRI system (Signa Excite; GE Healthcare, USA) using a custom-made Tx/Rx radio-frequency coil. SD rats were anesthetized by intraperitoneal injections of xylazine (10 mg/kg) and ketamine (100 mg/kg), positioned on a cradle heated by temperature-controlled water, and given Gd-EOB-DTPA or Gd-DTPA-Pullulan into their tail vein via a pre-inserted catheter. The injection dose was 0.05 mmol/kg of Gd. Dynamic contrast-enhanced T1-weighted MR images (TR = 200 ms, TE = 3.2 ms, flip angle = 80°, slice thickness = 1.5 mm) were recorded for 30 min.

2.7. Statistical analysis

Levels of statistical significance between two unpaired treatments were assessed by Student's *t*-test. A p value of less than 0.05 was regarded as statistically significant. The data are expressed as mean ± standard deviation (SD).

3. Results

3.1. Synthesis of Gd-DTPA-Pullulan

The chemical structure of Gd-DTPA-Pullulan is depicted in Fig. 1. The conjugation was confirmed by zeta potential and Fourier transform infrared (FT-IR) spectroscopy. The estimated zeta potential of pullulan was −1.5 ± 0.8 mV. After modification with DTPA, the zeta potential decreased to −15.0 ± 3.0 mV. The zeta potential reversed back to 2.9 ± 0.9 mV when Gd^{3+} ions were conjugated with DTPA in the DTPA-Pullulan. The Gd-DTPA-Pullulan was further characterized by FT-IR. The absorption peaks at 3390 cm^{-1}, 2930 cm^{-1}, 1643 cm^{-1}, and 1023 cm^{-1} were assigned to O–H, C–H, O–C–O, and C–O stretching of pullulan. The ester linkage between DTPA and pullulan was verified by C = O at 1734 cm^{-1}. After complexation of Gd^{3+} ions to DTPA-Pullulan, the absorption peak at 1734 cm^{-1} was shifted to 1597 cm^{-1}, as shown in Fig. 2.

3.2. Content of residual free Gd^{3+} in Gd-DTPA-Pullulan

The content of free Gd^{3+} (residual Gd^{3+}) in Gd-DTPA-Pullulan after synthesis was estimated. Fig. 3A illustrates the absorption peaks of xylenol orange (a colorimetric dye) at 433 and 573 nm. In the absence of Gd^{3+} ions, the band at 433 nm is more intense than that at 573 nm.

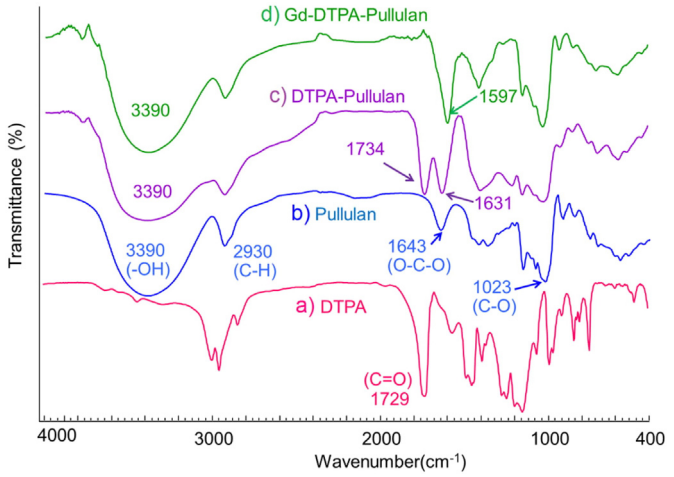

Fig. 2. FTIR spectra of (a) diethylene triamine pentaacetic dianhydride (DTPA), (b) pullulan, (c) pullulan modified with DTPA (DTPA-Pullulan), and (d) pullulan-conjugated gadolinium diethylene triamine pentaacetate (Gd-DTPA-Pullulan). The band at 1734 cm^{-1} supported the ester linkage formation of DTPA and pullulan. The shift of a band from 1734 cm^{-1} to 1597 cm^{-1} is due to coordination between gadolinium and carboxylic group of DTPA.

On the other hand, when free Gd^{3+} ions are introduced the band intensity at 433 nm decreases whereas the band at 573 nm increases. Fig. 3B shows the solution color of Gd-DTPA-Pullulan and Gd-EOB-DTPA compared to that of free Gd^{3+} at various concentrations. The solution color changed from yellow to violet with higher Gd^{3+} concentration. The yellow color was observed for both Gd-DTPA-Pullulan and Gd-EOB-DTPA. Thus, less than 0.01 wt.% of residual Gd^{3+} resided in Gd-

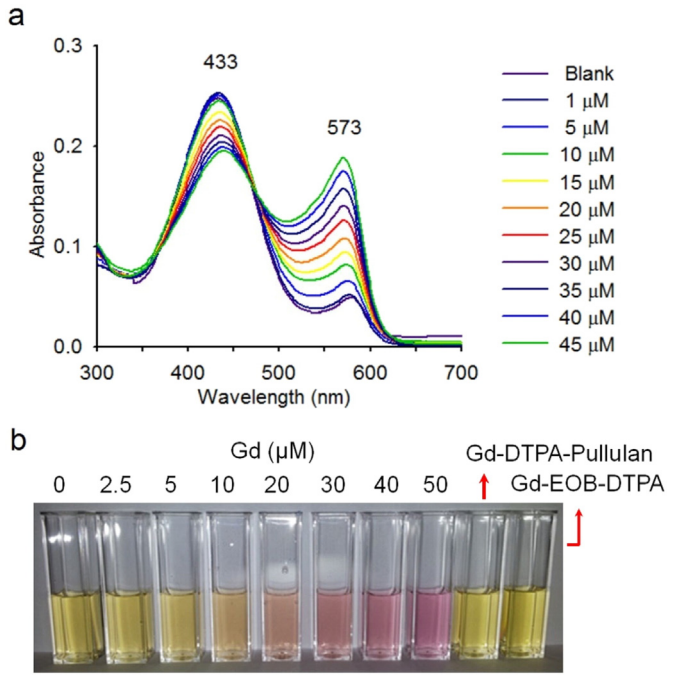

Fig. 3. (a) Absorbance of xylenol orange with various gadolinium concentrations (0–45 μM). The increase of gadolinium concentration causes a decrease of the band intensity at 433 nm and increase of the band at 573 nm. (b) Color change photographs of pure xylenol orange solution, xylenol orange in the presence of various gadolinium concentrations (2.5–50 μM), and xylenol orange in the presence of Gd-DTPA-Pullulan and Primovist (Gd-EOB-DTPA). The color changed from yellow to pink due to the complexation of gadolinium and xylenol orange. The color of xylenol orange after Gd-DTPA-Pullulan and Gd-EOB-DTPA adding did not change because of less gadolinium binding with xylenol orange. (For interpretation of the references to color in this figure legend, the reader is referred to the web version of this article.)

DTPA-Pullulan, a value that is relatively smaller than the reported free Gd content of commercial Gd-based contrast agent [19]. We found that addition of extra DTPA effectively removed the residual Gd^{3+} in the Gd-DTPA-Pullulan samples.

3.3. Release of transmetalated Gd^{3+}

The transmetalation study between Gd^{3+} and Ca^{2+} as well as Fe^{2+} ions was performed in dialysis membrane. Samples were collected from 1 to 8 h and introduced into an ICP-OES. The amount of Gd^{3+} released by co-incubation with Ca^{2+} at 8 h was approximately 1.0 ± 0.51%, whereas Gd-EOB-DTPA released 2.65 ± 1.50% of Gd^{3+} in total ($p < 0.05$), as shown in Fig. 4. In the case of Gd-DTPA-Pullulan with Ca^{2+} ions, the percent exchange of Gd^{3+} ions was only 0.2% after 2 h incubation. The transmetalation of Gd-DTPA-Pullulan occurred at moderate rates. Gd-DTPA-Pullulan also showed the good chelation stability against Fe^{2+}. Co-incubation with Fe^{2+} shown only 0.00046% (5 ppm) of Gd^{3+} was released at 8 h (Fig. S2).

3.4. Plasma and tissue concentration

Fig. 5 displays the plasma concentration–time profiles of Gd-DTPA-Pullulan and Gd-EOB-DTPA after mouse tail vein injection. Gd-DTPA-Pullulan showed extended plasma circulation compared with Gd-EOB-DTPA. Both agents showed typical bi-exponential decay of plasma concentration (i.e., rapid distribution and slow elimination). The concentration of Gd-DTPA-Pullulan and Gd-EOB-DTPA at 1 h after injection was 69.44 ± 12.64 g/mL and 3.77 ± 0.48 ng/mL, respectively. The biological half-life at alpha-phase was 0.43 ± 0.07 h and 0.11 ± 0.002 h for Gd-DTPA-Pullulan and Gd-EOB-DTPA (Table 1).

Tissue distribution of Gd-DTPA-Pullulan and Gd-EOB-DTPA is shown in Fig. 6. Gd- showed high accumulation in liver and kidney at 3 h and 24 h. In contrast, Gd-DTPA-Pullulan exhibited higher accumulation in spleen and liver, and the accumulation in liver was prolonged up to 24 h. These data strongly suggest that Gd-DTPA-Pullulan affords a prolonged MR acquisition window for the vascular system and abdominal tissues (e.g., liver) more than 30 min after injection.

3.5. Enhanced MR contrast and prolonged MR acquisition time

Fig. 7 illustrates the coronal-plane abdominal images of normal rats. Especially in the abdominal region (liver vessels), Gd-DTPA-Pullulan exhibited higher T1 contrast than Gd-EOB-DTPA and sustained the initial contrast more than 30 min (Fig. 7b). Generally Gd-DTPA-Pullulan provided more distinct abdominal MR imaging than Gd-EOB-DTPA both initially and 30 min after injection.

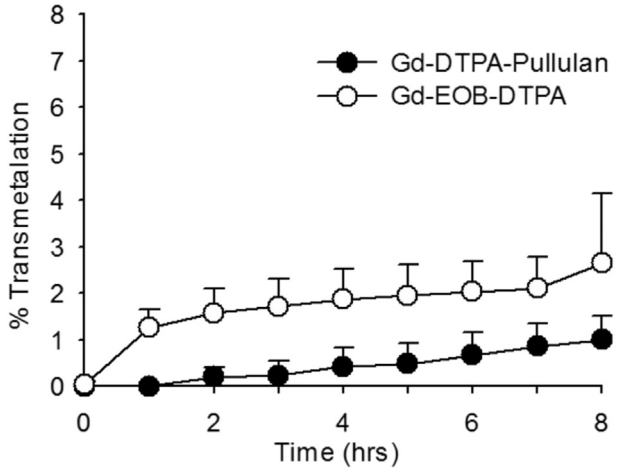

Fig. 4. Transmetalation of free gadolinium ions from Gd-DTPA-Pullulan (fill circle) and Gd-EOB-DTPA (open circle) under incubation with 1 mM $CaCl_2$.

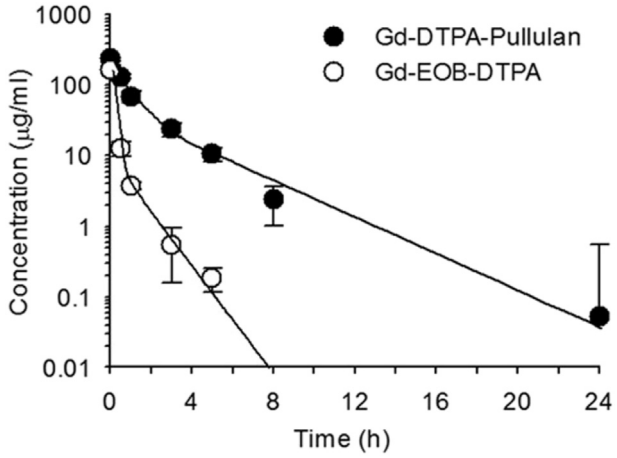

Fig. 5. Plasma gadolinium concentration versus time profiles of pullulan-conjugated gadolinium diethylene triamine pentaacetate (Gd-DTPA-Pullulan) (fill circle) and Primovist (Gd-EOB-DTPA) (open circle) after intravenous injection at a dose of 0.1 mmol Gd/kg. The plasma gadolinium concentration of Gd-DTPA-Pullulan showed the extended blood circulation which suggested the possible application for blood-pooling MR imaging agent.

4. Discussion

Successful synthesis of Gd-DTPA-Pullulan was confirmed via FT-IR and zeta potential. The zeta potential of pullulan decreased when it was chemically modified with DTPA due to introduction of the carboxyl groups of DTPA to the molecules of pullulan. Gd^{3+} ions were chelated to those carboxylate groups of DTPA via coordination, leading to zeta potential reversal through neutralization of the charge of DTPA components. The ester linkage observed by FT-IR supported the formation between DTPA and pullulan. The shift of the carbonyl absorption peak (C = O) to a lower wave number suggested that coordination between carboxylate groups of DTPA and Gd^{3+} ions had occurred.

The residual free Gd^{3+} was then evaluated by colorimetric method using xylenol orange. The presence of free Gd^{3+} produced a violet color observed visually. In the Gd-DTPA-Pullulan samples, the residual free Gd^{3+} was less than 0.01 wt.%. This result implied that our synthesis of Gd-DTPA-Pullulan reliably controlled the residual free Gd^{3+} and that Gd-DTPA-Pullulan was safe and would not generate false positive signals in the body.

In-body metal ions including Fe^{2+}, Zn^{2+}, Cu^{2+}, and Ca^{2+} exchange Gd^{3+} in DTPA, and the release of Gd^{3+} increases the risk of nephrogenic systemic fibrosis and dermopathy [2,6,20]. Cacheris et al. studied the transmetalation of Gd^{3+} ions in the body and reported that Cu^{2+} ions had very high affinity for the complexes, yet were present at low concentration (1–10 μM) in the blood [21]. In this study, Ca^{2+} and Fe^{2+},

Table 1
Summary of pharmacokinetic parameters of Gd-DTPA-Pullulan and Gd-EOB-DTPA after intravenous injection into normal mice. Values are means ± S.D.

	Gd-DTPA-Pullulan	Gd-EOB-DTPA
AUC (last), (μg * h/ml)	280.59 ± 28.33	36.98 ± 0.53
$T_{1/2,\ alpha}$ (h)	0.43 ± 0.07	0.11 ± 0.002
$T_{1/2,\ beta}$ (h)	2.32 ± 1.21	0.79 ± 0.09
AUMC (μg * h^2/ml)	611.19 ± 284.17	15.15 ± 1.44
MRT (h)	2.17 ± 0.81	0.41 ± 0.03
V_{ss} (ml/kg)	122.07 ± 34.97	174.17 ± 11.80
CL (ml/h/kg)	56.0 ± 5.66	425.1 ± 6.11

AUC; area under the curve, AUMC; area under the first moment curve, MRT; mean resident time, Vss; volume of distribution at steady state, CL; clearance.

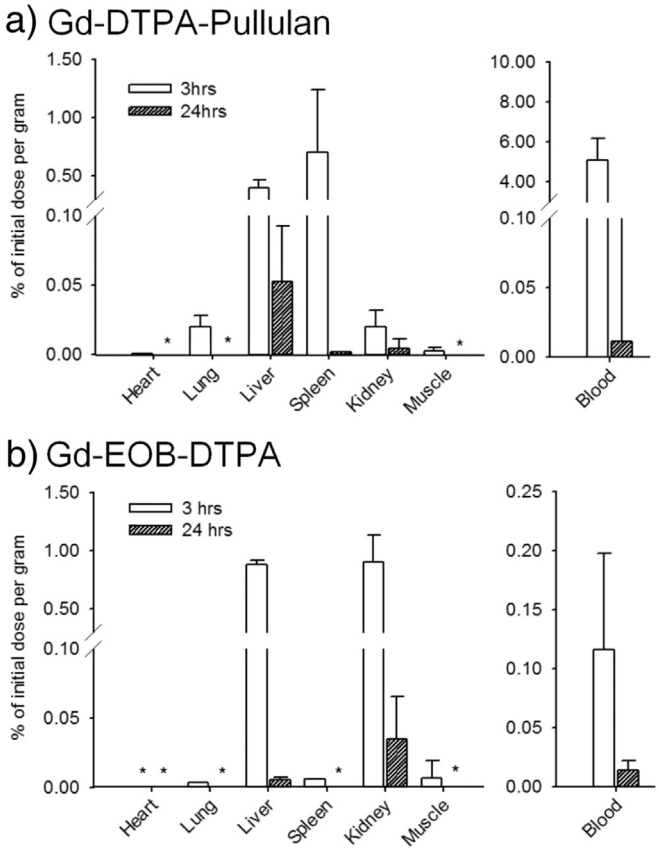

Fig. 6. Tissue and blood distribution of gadolinium after intravenous injection of Gd-DTPA-Pullulan (a) and Gd-EOB-DTPA (b), respectively; 3 h (open bar), 24 h (fill bar). The accumulation of gadolinium in liver and spleen was higher than that in other tissues in the case of Gd-DTPA-Pullulan injection, whereas for Gd-EOB-DTPA injection, the gadolinium was accumulated in liver and kidney. *; under the limit of detection.

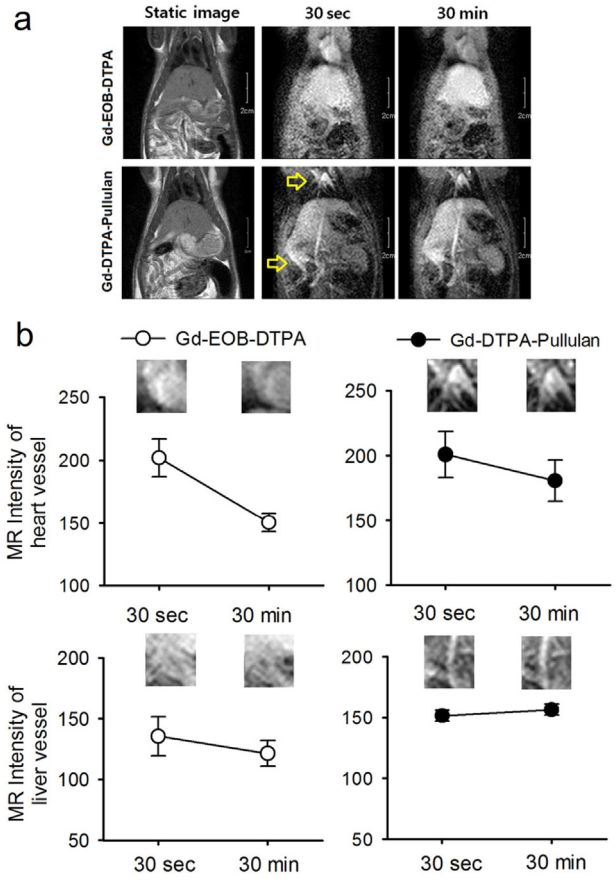

Fig. 7. (a) The abdominal MR images of rat after intravenous injection of Gd-EOB-DTPA (upper) and Gd-DTPA-Pullulan (lower). (b) Intensity of region of interest (ROI) of Gd-EOB-DTPA and Gd-DTPA-Pullulan in heart region and abdominal vessel at 30 s and 30 min.

the most abundant metal ion in the body, was selected as a competitive ion rather than Zn^{2+} and Cu^{2+}. The reported concentration of serum calcium is 2.25–2.5 mmol/L. Moreover, $Fe^{2+/3+}$ is the most abundant metal ion in the circulating blood (red blood cells). We proved Gd-DTPA-Pullulan possessed much higher chelation stability than Gd-EOB-DTPA (Figs. 4 and S2). Frenzel et al. reported that the percent transmetalation of Gd-EOB-DTPA was approximately 1.5% in serum with 10 mM phosphate buffer for 15 days [19]. Our experiment was performed at high concentration of Ca^{2+} ions, and 1.0 ± 0.51% of transmetalation was a considerably safer than that in the reported data [19]. However, the longer half-life of Gd-DTPA-Pullulan paradoxically increases the chance of transmetalation in the body. In this study, we did not estimate the free Gd^{3+} in the blood or tissues during the animal study. We just, therefore, interpret the extent of transmetalation in the body based on the pharmacokinetic parameters. The mean resident time (MRT) of Gd-DTPA-Pullulan and Gd-EOB-DTPA was 2.17 ± 0.81 and 0.41 ± 0.03 h, respectively (Table 1). Gd-DTPA-Pullulan showed approximately 5.3 folds higher body retention than Gd-EOB-DTPA. The extent of transmetalation at the MRT was 0.21% and 0.48% for Gd-DTPA-Pullulan and Gd-EOB-DTPA, respectively (Fig. 4). Based on this observation, we can suggest Gd-DTPA-Pullulan probably keeps lower extent of transmetalation during the circulation in the body.

The kidney is the major elimination organ of Gd-chelating agents, but Gd-EOB-DTPA typically undergoes both hepatic and renal elimination [22]. Our data also showed higher accumulation of Gd-EOB-DTPA in liver and kidney. Interestingly, Gd-DTPA-Pullulan displayed higher accumulation in liver and spleen than kidney at 3 h after the injection and showed prolonged accumulation in liver until 24 h (Fig. 6). Yamaoka et al. reported that more than 40% of the injected pullulan (100 k of m.w.) accumulated in the liver [23]. Pullulan has specific affinity for asialoglycoproteins, which are abundantly expressed on the sinusoidal surface of hepatocytes. So, Gd-DTPA-Pullulan has a potential for abdominal MR imaging, especially for liver, and our data also strongly support this observation.

The instantaneous distribution and elimination of contrast agents allow very short time windows for MR imaging, especially for vascular imaging. Dynamic contrast-enhanced MR (DCE-MR) is performed from 2 to 15 s to 5–10 min post-injection [24–27]. MR imaging of vascular vessels, i.e., cerebral, cardiac and hepatic vessels, demonstrates rapid, short contrast enhancement followed by a fairly fast washout. In the case of hepatic tumor, MR imaging is taken during the arterial phase (25–30 s post-injection), specifically the late hepatic arterial phase, when the portal vein is only slightly enhanced (60–80 s post-injection). Therefore, extended blood retention of MR agents could be very helpful in obtaining more distinct diagnostic images [28]. Gd-DTPA-Pullulan maintained the initial contrast intensity in heart and liver for at least 30 min after injection (Fig. 7B). This extended MR contrast power coincides with the plasma concentration profile of Gd-DTPA-Pullulan (Fig. 5). The data suggest that Gd-DTPA-Pullulan with prolonged blood retention and enhanced chelation stability eventually allows more precise diagnosis of abdominal vascular abnormalities.

5. Conclusion

Gd-DTPA-Pullulan was comparable to the commercial Gd-chelation MR imaging agents in the degree of free Gd^{3+} content (<0.01%). Gd-DTPA-Pullulan also showed longer blood circulation, liver retention and prolonged T1 contrast. Those data suggest that Gd-DTPA-Pullulan

is eligible for further preclinical and clinical development as a blood-pooling MR contrast agent.

Acknowledgments

This research was supported by the Basic Science Research Program through the National Research Foundation of Korea (NRF) funded by the Ministry of Science, ICT and Future Planning (NRF-2014K2A2A2000720) and (2014R1A2A2A04006562).

Appendix A. Supplementary data

Supplementary data to this article can be found online at http://dx.doi.org/10.1016/j.msec.2016.01.008.

References

[1] P. Caravan, J.J. Ellison, T.J. McMurry, R.B. Lauffer, Gadolinium(III) chelates as MRI contrast agents: structure, dynamics, and applications, Chem. Rev. 99 (1999) 2293–2352.
[2] S.A. Greenberg, Zinc transmetallation and gadolinium retention after MR imaging: case report, Radiology 257 (2010) 670–673.
[3] T. Grobner, Gadolinium—a specific trigger for the development of nephrogenic fibrosing dermopathy and nephrogenic systemic fibrosis? Nephrol. Dial. Transplant. 21 (2006) 1104–1108.
[4] P. Marckmann, L. Skov, K. Rossen, A. Dupont, M.B. Damholt, J.G. Heaf, H.S. Thomsen, Nephrogenic systemic fibrosis: suspected causative role of gadodiamide used for contrast-enhanced magnetic resonance imaging, J. Am. Soc. Nephrol. 17 (2006) 2359–2362.
[5] M.A. Perazella, R.F. Reilly, Nephrogenic systemic fibrosis: recommendations for gadolinium-based contrast use in patients with kidney disease, Semin. Dial. 21 (2008) 171–173.
[6] A.D. Sherry, P. Caravan, R.E. Lenkinski, Primer on gadolinium chemistry, J. Magn. Reson. Imaging 30 (2009) 1240–1248.
[7] K.J. Murphy, J.A. Brunberg, R.H. Cohan, Adverse reactions to gadolinium contrast media: a review of 36 cases, AJR Am. J. Roentgenol. 167 (1996) 847–849.
[8] M.F. Bellin, MR contrast agents, the old and the new, Eur. J. Radiol. 60 (2006) 314–323.
[9] C.F. Geraldes, S. Laurent, Classification and basic properties of contrast agents for magnetic resonance imaging, Contrast Media Mol. Imaging 4 (2009) 1–23.
[10] K.N. Raymond, V.C. Pierre, Next generation, high relaxivity gadolinium MRI agents, Bioconjug. Chem. 16 (2005) 3–8.
[11] M.F. Silva, L.P. Fernandez, R.A. Olsina, Monitoring the elimination of gadolinium-based pharmaceuticals. Cloud point preconcentration and spectrophotometric determination of Gd(III)-2-(3,5-dichloro-2-pyridylazo)-5-dimethylaminophenol in urine, Analyst 123 (1998) (1803-1807).
[12] M.N. Eakins, S.M. Eaton, R.A. Fisco, R.J. Hunt, C.E. Ita, T. Katona, L.M. Owies, E. Schramm, J.W. Sulner, C.W. Thompson, et al., Physicochemical properties, pharmacokinetics, and biodistribution of gadoteridol injection in rats and dogs, Acad. Radiol. 2 (1995) 584–591.
[13] Y. Feng, Y. Zong, T. Ke, E.K. Jeong, D.L. Parker, Z.R. Lu, Pharmacokinetics, biodistribution and contrast enhanced MR blood pool imaging of Gd-DTPA cystine copolymers and Gd-DTPA cystine diethyl ester copolymers in a rat model, Pharm. Res. 23 (2006) 1736–1742.
[14] T. Staks, G. Schuhmann-Giampieri, T. Frenzel, H.J. Weinmann, L. Lange, J. Platzek, Pharmacokinetics, dose proportionality, and tolerability of gadobutrol after single intravenous injection in healthy volunteers, Investig. Radiol. 29 (1994) 709–715.
[15] C.H. Huang, A. Tsourkas, Gd-based macromolecules and nanoparticles as magnetic resonance contrast agents for molecular imaging, Curr. Top. Med. Chem. 13 (2013) 411–421.
[16] H. Yim, S.G. Yang, Y.S. Jeon, I.S. Park, M. Kim, D.H. Lee, Y.H. Bae, K. Na, The performance of gadolinium diethylene triamine pentaacetate-pullulan hepatocyte-specific T1 contrast agent for MRI, Biomaterials 32 (2011) 5187–5194.
[17] B. Hamm, T. Staks, A. Muhler, M. Bollow, M. Taupitz, T. Frenzel, K.J. Wolf, H.J. Weinmann, L. Lange, Phase I clinical evaluation of Gd-EOB-DTPA as a hepatobiliary MR contrast agent: safety, pharmacokinetics, and MR imaging, Radiology 195 (1995) 785–792.
[18] A. Barge, G. Cravotto, E. Gianolio, F. Fedeli, How to determine free Gd and free ligand in solution of Gd chelates. A technical note, Contrast Media Mol. Imaging 1 (2006) 184–188.
[19] T. Frenzel, P. Lengsfeld, H. Schirmer, J. Hutter, H.J. Weinmann, Stability of gadolinium-based magnetic resonance imaging contrast agents in human serum at 37 degrees C, Investig. Radiol. 43 (2008) 817–828.
[20] Z. Jaszberenyi, I. Banyai, E. Brucher, R. Kiraly, K. Hideg, T. Kalai, Equilibrium and NMR studies on GdIII, YIII, CuII and ZnII complexes of various DTPA-N,N″-bis(amide) ligands. Kinetic stabilities of the gadolinium(III) complexes, Dalton Trans. (2006) 1082–1091.
[21] W.P. Cacheris, S.C. Quay, S.M. Rocklage, The relationship between thermodynamics and the toxicity of gadolinium complexes, Magn. Reson. Imaging 8 (1990) 467–481.
[22] H.J. Weinmann, G. Schuhmann-Giampieri, H. Schmitt-Willich, H. Vogler, T. Frenzel, H. Gries, A new lipophilic gadolinium chelate as a tissue-specific contrast medium for MRI, Magn. Reson. Med. 22 (1991) 233–237 (discussion 242).
[23] T. Yamaoka, Y. Tabata, Y. Ikada, Body distribution profile of polysaccharides after intravenous administration, Drug Deliv. 1 (1993) 75–82.
[24] V.L. Nguyen, M.E. Kooi, W.H. Backes, R.H. van Hoof, A.E. Saris, M.C. Wishaupt, F.A. Hellenthal, R.J. van der Geest, A.G. Kessels, G.W. Schurink, T. Leiner, Suitability of pharmacokinetic models for dynamic contrast-enhanced MRI of abdominal aortic aneurysm vessel wall: a comparison, PLoS One 8 (2013), e75173.
[25] B. Turkbey, D. Thomasson, Y. Pang, M. Bernardo, P.L. Choyke, The role of dynamic contrast-enhanced MRI in cancer diagnosis and treatment, Diagn. Interv. Radiol. 16 (2010) 186–192.
[26] A. Phinikaridou, M.E. Andia, S. Lacerda, S. Lorrio, M.R. Makowski, R.M. Botnar, Molecular MRI of atherosclerosis, Molecules 18 (2013) 14042–14069.
[27] C. Nolte-Ernsting, G. Adam, A. Bucker, S. Berges, A. Bjornerud, R.W. Gunther, Abdominal MR angiography performed using blood pool contrast agents: comparison of a new superparamagnetic iron oxide nanoparticle and a linear gadolinium polymer, AJR Am. J. Roentgenol. 171 (1998) 107–113.
[28] A.J. van der Molen, M.F. Bellin, Extracellular gadolinium-based contrast media: differences in diagnostic efficacy, Eur. J. Radiol. 66 (2008) 168–174.